Ferromagnetism of two-flavor quark matter in chiral and/or color-superconducting phases at zero and finite temperatures

M. Inui, H. Kohyama, A. Niégawa

Graduate School of Science, Osaka City University,

Sumiyoshi-ku, Osaka 558-8585, JAPAN

(Dated: Received today)

Abstract

We study the phase structure of the unpolarized and polarized two-flavor quark matters at zero and finite temperatures within the Nambu–Jona-Lasinio (NJL) model. We focus on the region, which includes the coexisting phase of quark-antiquark and diquark condensates. Generalizing the NJL model so as to describe the polarized quark matter, we compute the thermodynamic potential as a function of the quark chemical potential (μ), the temperature (T), and the polarization parameter. The result heavily depends on the ratio G_D/G_S, where G_S is the quark-antiquark coupling constant and G_D is the diquark coupling constant. We find that, for small G_D/G_S, the "ferromagnetic" phase is energetically favored over the "paramagnetic" phase. On the other hand, for large G_D/G_S, there appears the window in the (μ, T)-plane, in which the "paramagnetic" phase is favored.

PACS numbers: 11.10.Wx, 11.30.Qc, 11.30.Rd.

I. INTRODUCTION

Quantum chromodynamics (QCD) is the fundamental theory of strong interaction between quarks and gluons. QCD is an asymptotically free theory and perturbation theory may be used at high density and/or temperature. One-gluon exchange interaction between two quarks in the color antitriplet channel is attractive. Then one expects that a quark matter undergoes a phase transition to color superconducting phases at high density and relatively low temperature. Around two decades ago, it was shown that such phase transitions really take place at high density and low temperature [1]. Around a decade ago, it was found [2] that the color superconducting gaps are of $O(100\mathrm{MeV})$, which are comparable with nuclear matter density.

Quark matter is expected to be produced in heavy-ion-collision experiments, and might exist inside compact stars. If quark stars exist, they are quark matters in itself. Such quark matters are the system with intermediate density at low temperature, so that perturbative QCD is not applicable. Although lattice QCD is powerful for studying the system with vanishing net baryon density, it is not efficient, at the present moment, for studying nonzero baryon density systems due to the "sign problem". Then, for studying such systems, one should rely on some effective theories of QCD, such as the extended Nambu–Jona-Lasinio (NJL) model [3]. The NJL model incorporates above-mentioned attractive nature of the one-gluon exchange interaction between two quarks in the color antitriplet channel. Furthermore, it successfully describes static properties of the pion (e.g., pion mass and decay constant) in the hadoronic phase through chiral phase transition (see, e.g., [4]).

Theoretical studies using the extended NJL model as well as other approaches have disclosed possible existence of various color superconducting phases; regular 2SC phase, charge-neutral gapless 2SC phase, color-flavor-locked phase, and so on. Furthermore, it has been found that, at moderate baryon density region, the chiral and diquark condensates co-exist [5]. (For recent reviews, see, e.g., [6, 7].)

Magnetic property of quark matter is yet another important issue. Tatsumi was the first who pointed out the possible instability of a quark matter against the spin polarization (ferromagnetism) [8]: Within the one-gluon-exchange approximation in QCD, he computed the energy density $\mathcal{E}$ of quark matter at zero temperature as a function of polarization parameter p, and found that, at relatively low density, $\mathcal{E}(p)$ decreases as p increases. Since

then, there appear quite a few papers that are devoted to possible ferromagnetism in quark matter [9].

In this paper, we generalize the Tatsumi's analysis [8] to the case of polarized two-flavor quark matters with moderate baryon density at zero and finite temperatures. We introduce two types of polarized quark matters; the one is the "magnetic-moment–polarized" quark matters and the other is the "spin-polarized" quark matters. For dealing with such systems, we generalize the extended NJL model and employ the mean-field or Hartree approximation.

In Sec. II, we briefly describe the extended NJL model and generalize it so as to deal with polarized quark matters. In Sec. III, we derive the thermodynamic potential Ω for the two types of polarized quark matters at finite temperature within the mean field approximation. (Concrete derivation is given in Appendix D.) We find that the thermodynamic potentials for two types of polarized quark matters are of the same form. Difference may arise when the residual interactions are taken into account. In Sec. IV, we present the results obtained through numerical analysis. As in various analyses within the extended NJL model, the results are sensitive to the quark-antiquark coupling constant G_S and the diquark coupling constant G_D. We show that, in the case of $G_D/G_S \lesssim 1.15$, the polarized state is energetically favored. While, for $G_D/G_S \gtrsim 1.15$, there appears the window in a (μ, T)-plane, in which the unpolarized state is favored, where μ is the quark chemical potential and T is the temperature. Sec. V is devoted to summary and conclusion. In Appendix A, we briefly review the role of the projectors $\mathbf{P}_s^{(\tau)}$ ($\tau = \pm$, $s = \pm$), Eq. (2.5). In Appendix B, we show that the polarized quark numbers are conserved to the first order of coupling constants. In Appendix C, for completeness, we give the forms of the quark propagators in the polarized quark matters.

II. EXTENDED NAMBU–JONA-LASINIO MODEL AND ITS GENERALIZATION

A. Extended Nambu–Jona-Lasinio model

For describing the two-flavor quark matters, we adopt the extended Nambu–Jona-Lasinio model with the scalar-, pseudoscalar-, and scalar diquark-channels taken into account, whose

lagrangian density reads [7]

$$\mathcal{L} = \bar{q}\left(i\partial\!\!\!/ - m_0\right)q + G_S\left[(\bar{q}q)^2 + (\bar{q}i\gamma_5\vec{\tau}q)^2\right] + G_D\left[\left(i\bar{q}^C\epsilon\epsilon^b\gamma_5 q\right)\left(i\bar{q}\epsilon\epsilon^b\gamma_5 q^C\right)\right] ,$$

where m_0 is the current quark mass, $q^C = C\bar{q}^T$, $\bar{q}^C = q^T C$ with $C = i\gamma^2\gamma^0$ the charge-conjugation matrix. The quark field is a doublet in a flavor space and a triplet in a color space, $q \equiv q_{i\alpha}$ with $i = 1, 2$ and $\alpha =$ r(ed), g(reen), b(lue). The Pauli matrices $\vec{\tau} = (\tau^1, \tau^2, \tau^3)$ and $\epsilon \equiv i\tau^2$ act on the flavor space, while $(\epsilon^b)^{\alpha\beta} \equiv \epsilon^{\alpha\beta b}$ ($\epsilon^{rgb} = 1$) is a totally antisymmetric tensor in a color space. Although the coupling constants, G_S and G_D, enjoy the relation $G_D/G_S = 3/4$, we regard, as in [7], G_D/G_S as a free parameter.

B. Generalization to the case of polarized quark matter

For dealing with polarized quark matters, we first introduce a spin-polarization vector $n^\mu(\vec{p})$, which is obtained from its rest-frame form, $n^\mu(\vec{0}) = (0, \vec{e}^z) = (0, 0, 0, 1)$, through a Lorentz transformation [8],

$$n^0(\vec{p}) = \frac{\vec{p}\cdot\vec{e}^z}{m_0} , \qquad \vec{n}(\vec{p}) = \vec{e}^z + \frac{(\vec{p}\cdot\vec{e}^z)\,\vec{p}}{m_0(E_p + m_0)} . \tag{2.1}$$

Here E_p ($= \sqrt{p^2 + m_0^2}$) is the energy of the (anti)quark with momentum $\vec{p}$. Obviously, we have the relations,

$$n^2(\vec{p}) \equiv n_0^2(\vec{p}) - \vec{n}^{\,2}(\vec{p}) = -1 , \qquad E_p n_0(\vec{p}) = \vec{p}\cdot\vec{n}(\vec{p}) . \tag{2.2}$$

Using Eq. (2.1), we introduce a set of projectors onto the spin-polarized states:

$$\mathcal{P}_\pm(\vec{p}) = \frac{1}{2}\left(1 \pm \gamma_5 n\!\!\!/(\vec{p})\right) . \tag{2.3}$$

We also introduce a set of energy projectors [7]:

$$\tilde{\Lambda}_\pm(\vec{p}) = \frac{1}{2E_p}\left[E_p \pm \gamma_0\left(\vec{\gamma}\cdot\vec{p} - m_0\right)\right] . \tag{2.4}$$

It should be noted that $\gamma_0\tilde{\Lambda}_-(\vec{p}) = (m_0/E_p)\Lambda_+(\vec{p})$ and $\gamma_0\tilde{\Lambda}_+(-\vec{p}) = -(m_0/E_p)\Lambda_-(\vec{p})$, where $\Lambda_{+(-)}(\vec{p})$ is the projector onto the positive (negative) energy state. Now we introduce a set of projectors:

$$\mathbf{P}_s^{(+)}(\vec{p}) \equiv \mathcal{P}_s(\vec{p})\tilde{\Lambda}_+(\vec{p}) = \tilde{\Lambda}_+(\vec{p})\mathcal{P}_s(-\vec{p})$$

$$\mathbf{P}_s^{(-)}(\vec{p}) \equiv \mathcal{P}_s(-\vec{p})\tilde{\Lambda}_-(\vec{p}) = \tilde{\Lambda}_-(\vec{p})\mathcal{P}_s(\vec{p}) , \tag{2.5}$$

$$\mathbf{P}_s^{(\tau)}(\vec{p})\mathbf{P}_{s'}^{(\tau')}(\vec{p}) = \delta^{\tau\tau'}\delta_{ss'}\mathbf{P}_s^{(\tau)}(\vec{p}) , \qquad (\tau, \tau' = \pm,\ s, s' = \pm) . \tag{2.6}$$

In Appendix A, we show that, when acting on the quark field $q(x)$, $\mathbf{P}_{\pm}^{(-)}(i\nabla)$ projects out onto the "spin-up" ("spin-down") positive energy-state, while $\mathbf{P}_{\pm}^{(+)}(i\nabla)$ projects out onto the "spin-up" ("spin-down") negative energy-state.

The projectors $\mathbf{P}_s^{(\pm)}(\vec{p})$ enjoy the following relations:

$$\gamma_0 \mathbf{P}_s^{(\pm)}(\vec{p})\gamma_0 \;=\; \mathbf{P}_s^{(\pm)}(-\vec{p})\,, \tag{2.7}$$

$$\gamma_5 \mathbf{P}_s^{(\pm)}(\vec{p})\gamma_5 \;=\; \mathbf{P}_{-s}^{(\mp)}(-\vec{p})\,, \tag{2.8}$$

$$C\left(\mathbf{P}_s^{(\pm)}(\vec{p})\right)^T C \;=\; -\mathbf{P}_s^{(\mp)}(\vec{p})\,. \tag{2.9}$$

We are now in a position to describe the "polarized" quark matter. From the above observation, we introduce the "spin up"/"spin down" quark number, $Q_{\pm}^{(-)}$, and the "spin up"/"spin down" antiquark number, $Q_{\pm}^{(+)}$, where

$$Q_s^{(\tau)} = \int d^3x\, \mathcal{Q}_s^{(\tau)} \equiv \int d^3x\, q^\dagger(x)\mathbf{P}_s^{(\tau)}(i\nabla)q(x) \qquad (\tau = \pm,\ s = \pm)\,.$$

1. Magnetic-moment-polarized quark matter

Since a "spin up" ("spin down") quark and a "spin down" ("spin up") antiquark feel the same electromagnetic force, we introduce two quark chemical potentials: μ_+ is conjugate to the net quark-number charge with "positive magnetic moment (MM)",

$$Q_+ \equiv Q_+^{(-)} + Q_-^{(+)} \ \left(\equiv \int d^3x\, \mathcal{Q}_+\right)\,, \tag{2.10}$$

and μ_- is conjugate to the net quark-number charge with "negative MM",

$$Q_- \equiv Q_-^{(-)} + Q_+^{(+)} \ \left(\equiv \int d^3x\, \mathcal{Q}_-\right)\,. \tag{2.11}$$

It can readily be shown that $[Q_+, Q_-] = 0$. We call the quark matter with $\mu_+ \neq \mu_-$ the "MM-polarized" quark matter. For dealing with such quark matters, the term that depends on μ_+ and μ_- should be added to the Lagrangian density;

$$\tilde{\mathcal{L}} \to \tilde{\mathcal{L}} + \mu_+\mathcal{Q}_+ + \mu_-\mathcal{Q}_-\,. \tag{2.12}$$

The polarized charges Q_+ and Q_- are not conserved. We show in Appendix B that they are conserved up to and including the first order of coupling constants G_S and G_D. It is to be noted in passing that, when the mean-field approximation is employed, even the unpolarized charge $Q_+ + Q_-$ turns out not to be conserved[1].

[1] We thank A. Oguri for discussion on this point.

2. Spin-polarized quark matter

We define "spin-polarized" quark matters by introducing two chemical potentials, μ_+ and μ_-: μ_+ is conjugate to $Q_+^{(-)} + Q_+^{(+)}$ ($\equiv Q'_+$) and μ_- is conjugate to $Q_-^{(-)} + Q_-^{(+)}$ ($\equiv Q'_-$). One can show that $\left[Q'_+, Q'_-\right] = 0$. In this case, the counterpart to Eq. (2.12) is

$$\tilde{\mathcal{L}} \to \tilde{\mathcal{L}} + \mu_+ \mathcal{Q}'_+ + \mu_- \mathcal{Q}'_- \,. \tag{2.13}$$

We see in Appendix B that the charges Q'_+ and Q'_- are conserved up to and including $O(G_S, G_D)$.

C. Mean field approximation

We employ the mean field approximation to get

$$\begin{aligned} \tilde{\mathcal{L}} \;=\; & \bar{q}\left(i\partial\!\!\!/ - m\right) q - \frac{1}{2}\Delta^{*b}\left(i\bar{q}^C \epsilon\epsilon^b \gamma_5 q\right) - \frac{1}{2}\Delta^b\left(i\bar{q}\epsilon\epsilon^b\gamma_5 q^C\right) \\ & -\frac{\sigma^2}{4G_S} - \frac{\Delta^{*b}\Delta^b}{4G_D}\,, \end{aligned} \tag{2.14}$$

where $\langle \bar{q} i\gamma_5 \vec{\tau} q\rangle = 0$ has been assumed [7] and

$$m \;=\; m_0 + \sigma = m_0 - 2G_S\langle\bar{\psi}\psi\rangle\,, \tag{2.15}$$

$$\Delta^b \;=\; -2G_D\langle i\bar{q}^C\epsilon\epsilon^b\gamma_5 q\rangle\,, \qquad \Delta^{*b} = -2G_D\langle i\bar{q}\epsilon\epsilon^b\gamma_5 q^C\rangle\,. \tag{2.16}$$

m in Eq. (2.15) is the constituent quark mass, which has received the contribution σ from the chiral condensate, if any. Then, when we use in the sequel various quantities defined in the last subsection, we replace the current quark mass m_0 with m.

From Eq. (2.14), we see that the red and green quarks participate in the diquark condensate, while the blue quarks do not.

III. THERMODYNAMIC POTENTIAL IN THE MEAN-FIELD APPROXIMATION

A. Magnetic-moment-polarized quark matter

Throughout in the sequel of this paper, we use the imaginary-time formalism. The grand partition function is defined by

$$\mathcal{Z} \;=\; \int \mathcal{D}\bar{q}\mathcal{D}q \exp\left\{\int_0^\beta d\tau \int d^3x \left(\tilde{\mathcal{L}}_E + \sum_{s=\pm}\mu_s \mathcal{Q}_s\right)\right\}, \tag{3.1}$$

where $\beta = 1/T$ is the inverse temperature, $\tau = ix^0$ $(0 < \tau < \beta)$ is the Euclidean time, and $\tilde{\mathcal{L}}_E = \tilde{\mathcal{L}}\big|_{x_0\,=\,-i\tau}$.

Since the exponent of Eq. (3.1) is bilinear in fields, $\mathcal{Z}$ is factorized as

$$\mathcal{Z} = \mathcal{Z}_{\rm const}\mathcal{Z}_b\mathcal{Z}_{r,g}\,. \tag{3.2}$$

$\mathcal{Z}_{\rm const}$ reads

$$\ln \mathcal{Z}_{\rm const} = -V\beta\left(\frac{\sigma^2}{4G_S} + \frac{\Delta^{b*}\Delta^b}{4G_D}\right), \tag{3.3}$$

where V is the volume of the system. The contribution from the blue quarks is

$$\mathcal{Z}_b = \int \mathcal{D}\bar{q}_b\mathcal{D}q_b \exp\left\{\int_0^\beta d\tau \int d^3x \left(\frac{1}{2}\bar{q}_b\left(G_0^+\right)^{-1}q_b + \frac{1}{2}\bar{q}_b^C\left(G_0^-\right)^{-1}q_b^C\right)\right\}, \tag{3.4}$$

where $[G_0^-(i\partial)]^{-1} = -C\left([G_0^+(-i\partial)]^{-1}\right)^T C$ and then

$$\left(G_0^\pm\right)^{-1} = i\partial\!\!\!/ - m \pm \gamma_0 \sum_{\tau,\,s=\pm}\mu_{\mp\tau s}\mathbf{P}_s^{(\tau)}(i\nabla)\,. \tag{3.5}$$

For the contribution from the red and green quarks, $Q = q_{r,g}$, we have

$$\begin{aligned}\mathcal{Z}_{r,\,g} \;=\; \int \mathcal{D}\bar{Q}\mathcal{D}Q \exp\left\{\int_0^\beta d\tau \int d^3x \left[\frac{1}{2}\bar{Q}\left(G_0^+\right)^{-1}Q\right.\right.\\ \left.\left. +\frac{1}{2}\bar{Q}^C\left(G_0^-\right)^{-1}Q^C + \frac{1}{2}\bar{Q}\Delta^- Q^C + \frac{1}{2}\bar{Q}^C\Delta^+ Q\right]\right\},\end{aligned} \tag{3.6}$$

where

$$\Delta^- = -i\Delta\epsilon\epsilon^b\gamma_5\,, \qquad \Delta^+ = -i\Delta^*\epsilon\epsilon^b\gamma_5\,. \tag{3.7}$$

We employ the Nambu-Gorkov formalism through introducing

$$\Psi_b \;=\; \begin{pmatrix} q_b \\ q_b^C \end{pmatrix}, \quad \bar{\Psi}_b = \begin{pmatrix}\bar{q}_b & \bar{q}_b^C\end{pmatrix},$$

$$\Psi \;=\; \begin{pmatrix} Q \\ Q^C \end{pmatrix}, \quad \bar{\Psi} = \begin{pmatrix}\bar{Q} & \bar{Q}^C\end{pmatrix}.$$

Going into a momentum space, we have (cf. Eq. (3.5))

$$\left(G_0^{\pm}\right)^{-1} = \sum_{\tau,\, s=\pm} \left(p_0 + \tau E_p \pm \mu_{\mp\tau s}\right) \gamma_0 \mathbf{P}_s^{(\tau)}(-\vec{p}) \,, \tag{3.8}$$

where

$$p_0 = i p_{0E} = \frac{i\pi}{\beta}(2n+1) \qquad (n = ..., -2, -1, 0, 1, 2, ...) \,. \tag{3.9}$$

Eqs. (3.4) and (3.6) turn out, in respective order, to

$$\begin{aligned} \mathcal{Z}_b &= \int \mathcal{D}\Psi_b \exp\left\{ \frac{1}{2} \sum_{n,\,\vec{p}} \bar{\Psi}_b \left(\beta G_0^{-1}\right) \Psi_b \right\} = \left[\mathrm{Det}\left(-\beta G_0^{-1}\right)\right]^{1/2} \,, \\ \mathcal{Z}_{r,g} &= \int \mathcal{D}\Psi \exp\left\{ \frac{1}{2} \sum_{n,\,\vec{p}} \bar{\Psi} \left(\beta G^{-1}\right) \Psi \right\} = \left[\mathrm{Det}\left(-\beta G^{-1}\right)\right]^{1/2} \,. \end{aligned}$$

Here

$$G_0^{-1} = \begin{pmatrix} \left(G_0^{+}\right)^{-1} \mathbf{1}_f & 0 \\ 0 & \left(G_0^{-}\right)^{-1} \mathbf{1}_f \end{pmatrix} \,, \quad G^{-1} = \begin{pmatrix} \left(G_0^{+}\right)^{-1} \mathbf{1}_f \mathbf{1}_c^{\perp} & \Delta^{-} \\ \Delta^{+} & \left(G_0^{+}\right)^{-1} \mathbf{1}_f \mathbf{1}_c^{\perp} \end{pmatrix} \,, \tag{3.10}$$

where $(\mathbf{1}_f)^{ij} = \delta^{ij}$ in the flavor space, and $(\mathbf{1}_c^{\perp})^{\alpha\beta} = \delta^{\alpha\beta} - \delta^{\alpha b}\delta^{\beta b}$ in the color space.

Although the forms of the propagators, G_0 and G, are not necessary for our purpose, we give them in Appendix C for completeness.

$\mathcal{Z}_b$ is obtained from $\mathcal{Z}_{r,g}$ by taking the limit, $\Delta = \Delta^* \to 0$;

$$\ln \mathcal{Z}_b = \frac{1}{2} \ln \mathcal{Z}_{r,g} \Big|_{\Delta\,=\,\Delta^*\,=\,0} \,. \tag{3.11}$$

Then we concentrate on evaluating $\mathcal{Z}_{r,g}$;

$$\ln \mathcal{Z}_{r,g} = \frac{1}{2} \ln \mathrm{Det}\left(-\beta G^{-1}\right) \,, \tag{3.12}$$

the computation of which is given in Appendix D.

Thermodynamic potential

From Eqs. (3.2), (3.3), (D.4) (cf. Eq. (D.3)), and Eq. (3.11), we obtain for the thermodynamic potential,

$$\begin{aligned} \Omega &= -\frac{T}{V} \ln \mathcal{Z} \\ &= \frac{\sigma^2}{4G_S} + \frac{|\Delta|^2}{4G_D} - N_f \int \frac{d^3p}{(2\pi)^3} \sum_{\rho,\,\sigma=\pm} \Big[E_{p,\,\rho}^{(\sigma)} + 2T \ln\left(1 + e^{-\beta E_{p,\,\rho}^{(\sigma)}}\right) \\ &\quad + \frac{1}{2} \left\{ E_{p,\,\rho}^{(\sigma)} + 2T \ln\left(1 + e^{-\beta E_{p,\,\rho}^{(\sigma)}}\right) \right\}_{\Delta=0} \Big] \,, \end{aligned} \tag{3.13}$$

where $N_f = 2$ is the number of flavor-degrees of freedom, and

$$E_{p,\,\rho}^{(\sigma)} = \left[\left(E_p + \sigma\frac{\mu_+ + \mu_-}{2}\right)^2 + |\Delta|^2\right]^{1/2} + \rho\frac{\mu_+ - \mu_-}{2}\,. \tag{3.14}$$

The three momentum integral in Eq. (3.13) is ultraviolet divergent, and, as usual, we introduce a momentum cut-off parameter Λ. The zero-temperature limit ($T \to 0$) of Ω reads

$$\Omega(T=0) = \frac{\sigma^2}{4G_S} + \frac{|\Delta|^2}{4G_D} - N_f \int \frac{d^3p}{(2\pi)^3} \sum_{\rho,\,\sigma=\pm} \left[\left|E_{p,\,\rho}^{(\sigma)}\right| + \frac{1}{2}\left|E_{p,\,\rho}^{(\sigma)}\right|_{\Delta\,=\,0}\right]\,. \tag{3.15}$$

Ω in Eqs. (3.13) and (3.15) yields the gap equations:

$$\frac{\partial\Omega}{\partial m} = 0\,, \qquad \frac{\partial\Omega}{\partial\Delta} = 0 \qquad (\Delta \equiv |\Delta|)\,. \tag{3.16}$$

A solution (m, Δ) to Eq. (3.16) is a local minimum point of Ω, when the following conditions are met:

$$\begin{aligned} &\frac{\partial^2\Omega}{\partial m^2}\frac{\partial^2\Omega}{\partial|\Delta^2|} - \left(\frac{\partial^2\Omega}{\partial m\partial\Delta}\right)^2 > 0\,, \\ &\frac{\partial^2\Omega}{\partial m^2} + \frac{\partial^2\Omega}{\partial|\Delta|^2} > 0\,. \end{aligned} \tag{3.17}$$

Polarized quark-number density

Let $n^{(\pm)}$ be the "positive (negative) magnetic moment" net quark-number density. $n^{(\pm)}$ is computed from Ω through partial differentiation with respect to $\mu_\pm$:

$$n^{(\pm)}(\mu_+, \mu_-, T) \;=\; -\frac{\partial\Omega}{\partial\mu_\pm} \quad \left(\equiv n_{r,\,g}^{(\pm)} + n_b^{(\pm)}\right)\,, \tag{3.18}$$

$$\begin{aligned} n_{r,\,g}^{(\pm)}(\mu_+, \mu_-, T) \;=\; & N_f \int \frac{d^3p}{(2\pi)^3}\theta(\Lambda - p) \sum_{\sigma=\pm}\left[\frac{\sigma E_{p,\,\sigma}}{\sqrt{E_{p,\,\sigma}^2 + |\Delta|^2}}\right. \\ & \left. - \sum_{\rho=\pm}\left(\frac{\sigma E_{p,\,\sigma}}{\sqrt{E_{p,\,\sigma}^2 + |\Delta|^2}} \pm \rho\right) n_F\left(E_{p,\,\rho}^{(\sigma)}\right)\right]\,, \end{aligned} \tag{3.19}$$

$$n_b^{(\pm)}(\mu_+, \mu_-, T) \;=\; N_f \int \frac{d^3p}{(2\pi)^3}\theta(\Lambda - p)\left[n_F(E_p - \mu_\pm) - n_F(E_p + \mu_\pm)\right]\,, \tag{3.20}$$

where $E_{p,\sigma} \equiv E_p + \sigma\bar{\mu}$ ($\bar{\mu} \equiv (\mu_+ + \mu_-)/2$) and $n_F(x) = 1/(e^{\beta x}+1)$ is the Fermi distribution function. In the limit $T \to 0$, $n^{(\pm)}$ turns out to

$$
\begin{aligned}
n_{r,\,g}^{(\pm)}(T=0) \;=\; & N_f \int \frac{d^3p}{(2\pi)^3}\theta(\Lambda - p) \\
& \times \left[\frac{\bar{\mu}+E_p}{\sqrt{(\bar{\mu}+E_p)^2+|\Delta|^2}} + \frac{\bar{\mu}-E_p}{\sqrt{(\bar{\mu}-E_p)^2+|\Delta|^2}} \right. \\
& -\theta\left(\frac{(\delta\mu)^2}{4} - |\Delta|^2\right)\,\theta\left(E_p - \bar{\mu} + \sqrt{\frac{(\delta\mu)^2}{4} - |\Delta|^2}\right) \\
& \left. \times \left(\frac{\bar{\mu}-E_p}{\sqrt{(\bar{\mu}-E_p)^2+|\Delta|^2}} \mp 1\right)\theta\left(\bar{\mu} + \sqrt{\frac{(\delta\mu)^2}{4} - |\Delta|^2} - E_p\right)\right] , \qquad (3.21) \\
n_b^{(\pm)}(T=0) \;=\; & N_f \int \frac{d^3p}{(2\pi)^3}\theta(\Lambda - p)\theta(\mu_\pm - E_p)\,, \qquad (3.22)
\end{aligned}
$$

where $\delta\mu \equiv \mu_+ - \mu_-$.

B. Spin-polarized quark matter

The counterpart to Eq. (3.8) is

$$
\left(G_0^{\pm}\right)^{-1} = \sum_{\tau,\,s=\pm} \left(p_0 + \tau E_p \pm \mu_s\right)\gamma_0 \mathbf{P}_s^{(\tau)}(-\vec{p})\,. \qquad (3.23)
$$

Ω is computed in a similar manner as in Appendix D and we obtain the same form as above, i.e., Eq. (3.13) with Eq. (3.14).

IV. NUMERICAL ANALYSIS

In this section, through numerical analyses, we will analyze the phase structure of the unpolaried and polarized quark matters at zero and finite temperatures. How the chiral condensate, diquark condensate, and the degree of polarization compete with one another will be discussed.

We first fix the parameters of the model as in [7]: The current quark mass $m_0 = 5.5$ MeV, the three-momentum cut-off $\Lambda = 0.637$ GeV, and the coupling constant $G_S = 5.32$ GeV^{-2}, which reproduces the properties of pion in vacuum. As mentioned above, although the standard value of G_D/G_S is 3/4, we leave it as a free parameter.

A. Unpolarized quark matter

1. $T = 0$

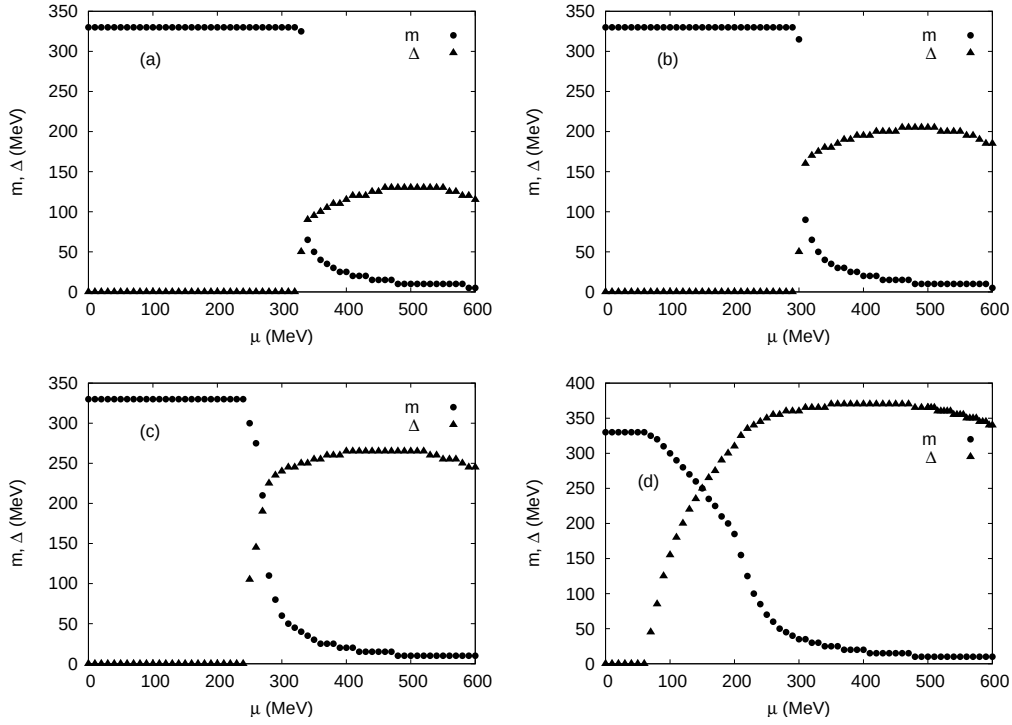

Fig. 1: Plots of m and Δ as functions of the chemical potential μ for $T = \delta\mu = 0$. (a), (b), (c), and (d) correspond to $G_D/G_s = 3/4$, 1.0, 1.2, and 1.5, respectively.

Throughout in the sequel of this section, values of all dimensionful quantities are given in unit of MeV. In [7], the two gaps m and $\Delta(\equiv |\Delta|)$ at $T = 0$ are displayed for various values of G_D/G_S. For completeness, we reproduce them in Fig. 1. The panel (a) corresponds to the standard value $G_D/G_S = 3/4$, while (b), (c) and (d) correspond, as in [7], to $G_D/G_S = 1.0, 1.2$, and 1.5, respectively. Close observation on Fig. 1 is given in [7], which we briefly recapitulate here.

Fig. 1 (a) ($G_D/G_S = 3/4$) shows that the chiral phase transition and the color superconducting (diquark) phase transition take place at nearly the same chemical potential $\mu_\chi \simeq \mu_\Delta \simeq 330$. These two phase transitions are of first order. There remains a small chiral condensate in the color superconducting (CSC) phase $\mu > \mu_\Delta$, which is a relic of the explicit chiral symmtery breaking ($m_0 \neq 0$).

We define μ_Δ, as usual, to be the value of the chemical potential at which the diquark condensate starts to appear. We define μ_χ to be the chemical potential at which m starts to decrease from nearly the constant value (rather than the chemical potential at which the chiral symmtery is restored). From Fig. 1 (b) - (d), we see that $\mu_\Delta \simeq \mu_\chi$ and, as G_D/G_S inceases, $\mu_\Delta \simeq \mu_\chi$ decreases. The chiral condensate in the coexistence phase is due to the dynamical symmtery breaking.

Here we like to add one finding. Within the accuracy of numerical computation, the value of μ at which the quark-number density, n, vanishes coincides with μ_Δ, i.e., $n(\mu, T = 0) = 0$ for $\mu \leq \mu_\Delta$.

2. $T \neq 0$

For the shake of copmarison to the case of $\delta\mu \neq 0$ in the next subsection, we display here the results for $T \neq 0$ and $\delta\mu = 0$.

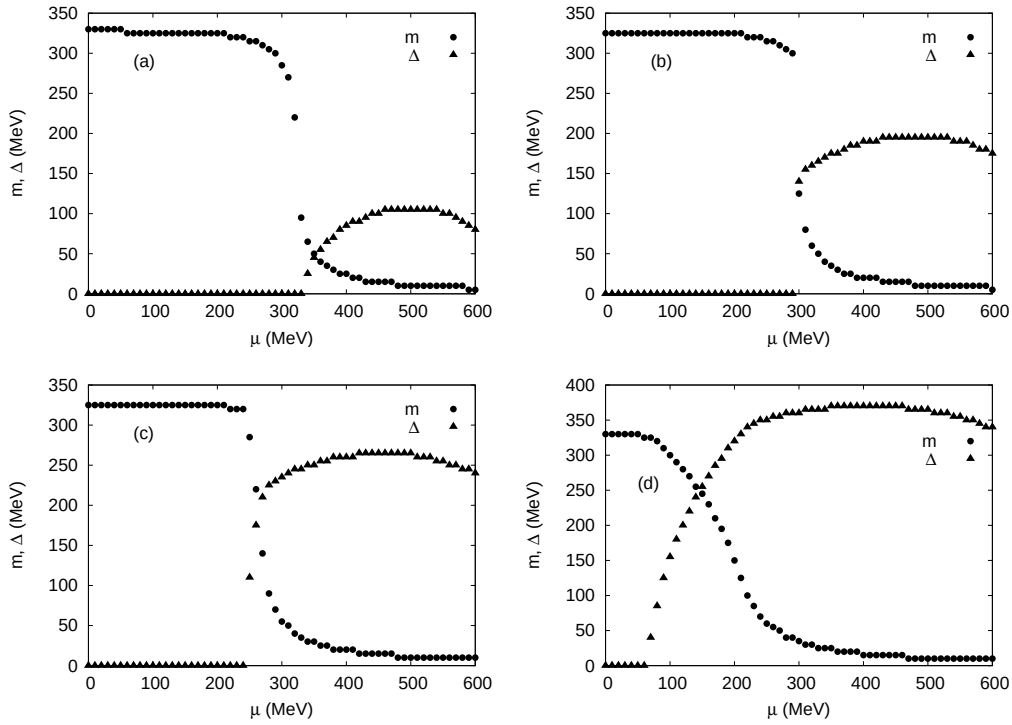

Fig. 2: The same as Fig. 1 for $T = 50$.

In Fig. 2, we plot m and Δ at $T = 50$ for the same values of G_D/G_S as in Fig. 1. Fig. 2 (a) shows that the value of μ_Δ is nearly the same as in the $T = 0$ case, and $\mu_\chi < \mu_\Delta$.

Both phase transitions are of second order. Δ in the region $\mu > \mu_\Delta$ is smaller than that in the $T = 0$ case. Comparing Fig. 1 (b) - (d) with Fig. 2 (b) - (d), we can make similar observation, besides that Δ's in the region $\mu > \mu_\Delta$ at $T = 50$ are not appreciably smaller than their $T = 0$ counterparts.

In the following we refer the region where $\Delta = 0$ ($m = O(m_0)$) to as the hadronic-phase (CSC-phase) region, while the region in between them *simply* to as the double-broken phase.

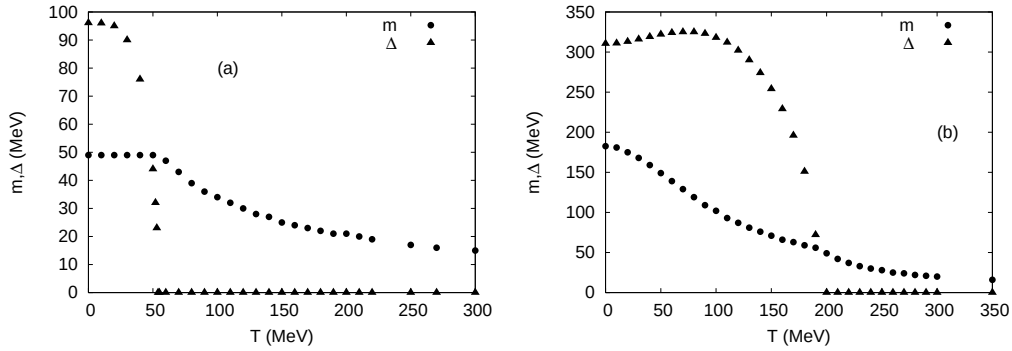

Fig. 3: m, Δ against T for (a) $(G_D/G_S, \mu) = (3/4, 350)$ and (b) $(G_D/G_S, \mu) = (1.5, 200)$.

Let us see the T dependence of m and Δ. In Fig. 3, choosing the double-broken phase region, we plot m and Δ against T. The panel (a) [(b)] corresponds to $G_D/G_S = 3/4$ [1.5] and $\mu = 350$ [200]. We see that Δ decreases as T increases and becomes zero at the critical temperature T_Δ. Above T_Δ, the color normal phase is realized. With respect to the chiral symmetry, the panel (a) shows that, as T increases, m starts to decrease at $T \simeq T_\Delta$, and the chiral symmetry is restored gradually. On the other hand, in the case of panel (b), m starts to decrease from the beginning ($T = 0$) and the chiral symmetry is restored gradually. We have observed the similar behavious for other values of μ.

Finally, in Fig. 4, we display the phase diagrams. The panels (a), (b), and (c) correpond to $G_D/G_S = 3/4$, 1.2, and 1.5, respectively.

B. Polarized quark matter

We have, among others, three parameters μ_+, μ_-, and T. We difine μ through

$$n_b^{(+)}(\mu_+, \mu_-, T)\Big|_{\mu_+ = \mu_- = \mu} = \frac{1}{6}\left[n^{(+)}(\mu_+, \mu_-, T) + n^{(-)}(\mu_+, \mu_-, T)\right], \tag{4.1}$$

where $n^{(\pm)}(\mu_+, \mu_-, T)$ is as in Eqs. (3.18) - (3.20). The procedure of numerical computation for various quantities goes as follows.

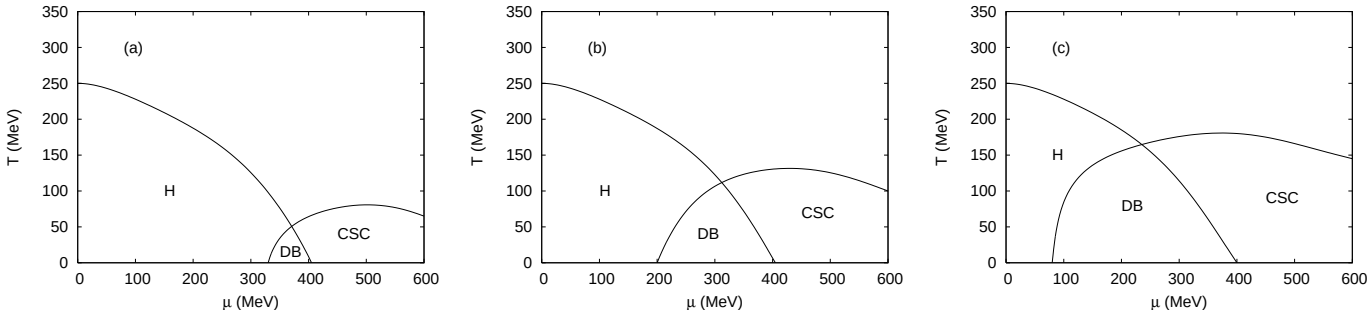

Fig. 4: Phase diagrams for $G_D/G_S = 3/4$ (a), 1.2 (b), and 1.5 (c).

H, CSC, and DB stand for hadronic, color-super-conducting, and double-broken phases, respectively.

1) We first fix T, $\mu(\geq 0)$, and $\mu_-(\geq 0)$.

2) Then, we solve two gap equatios, Eq. (3.16), and Eq. (4.1) simultaneously, and obtain the solution for (μ_+, m, Δ), and compute $\delta\mu = \mu_+ - \mu_-$.

3) Finally, we check if the two conditions (3.17) are met.

1. $\delta\mu$ dependence of m and Δ

Double-broken phase: We first study the parameter region where the unpolarized quark matter is in the double-broken phase. In Fig. 5, we plot m and Δ agaisnt $\delta\mu$ for different values of $(G_D/G_S,\ T,\ \mu)$: The panels (a), (b), (c), and (d) correspond to $(3/4, 0, 400)$, $(3/4, 50, 400)$, $(1.5, 0, 300)$, and $(1.5, 50, 300)$, respectively. Fig. 5 (a) shows that, as $\delta\mu$ increases, the first-order phase transition occurs at $\delta\mu = \delta\mu_p \simeq 220$. For $\delta\mu > \delta\mu_p$, the system is in the color normal phase. At $\delta\mu = \delta\mu_p$, a gap appears in m. Fig. 5 (b) shows similar behaviors as Fig. 5 (a) , but no gap appears in m at $\delta\mu = \delta\mu_p$. Figs. 5 (c) and (d) shows that, in the case of $G_D/G_S = 1.5$, both m and Δ are nearly independent of $\delta\mu$, and no phase transition occurs. We have carried out the same computation for different parameter values and found qualitatively the same results.

Hadronic phase: We study the parameter region where the unpolarized quark matter is in the hadronic phase. In Fig. 6, m and Δ are plotted against $\delta\mu$ for $(G_D/G_S, T, \mu) = (1.0, 50, 100)$ (cf. Fig. 2 (b)). We see that m and Δ $(= 0)$ are nearly independent of $\delta\mu$ and

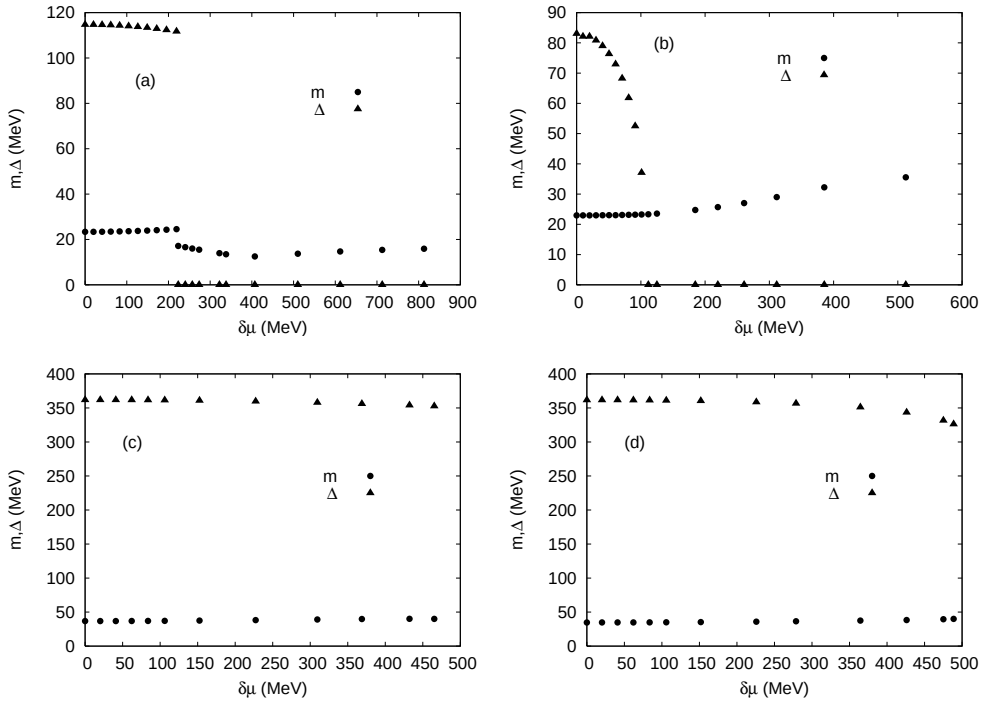

Fig. 5: m and Δ against $\delta\mu$. (a), (b), (c), and (d) correspond to (G_D/G_S, T, μ)=(3/4, 0, 400), (3/4, 50, 400), (1.5, 0, 300), and (1.5, 50, 300), respectively.

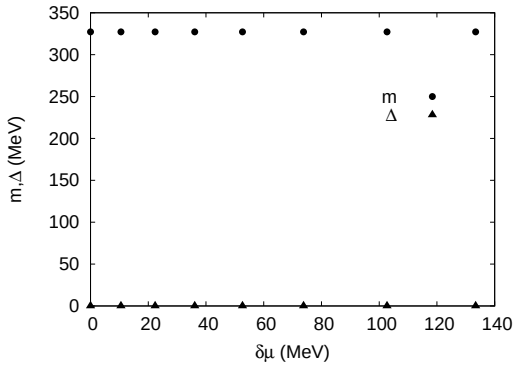

Fig. 6: m and Δ against $\delta\mu$ for (G_D/G_S, T, μ) =(1.0, 50, 100).

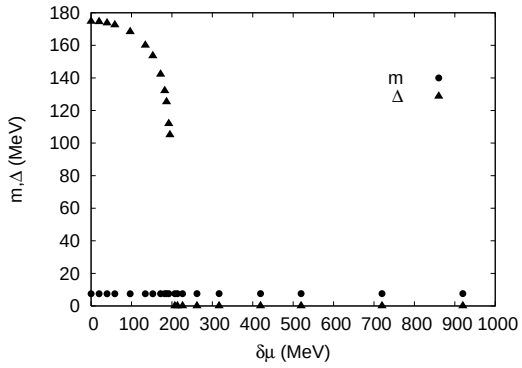

Fig. 7: m and Δ against $\delta\mu$ for (G_D/G_S, T, μ) =(1.0, 50, 600).

the quark matters are in the color normal phase for all $\delta\mu$. We have carried out the same computation choosing different parameter values and found qualitatively the same results.

CSC phase: Finally, we study the parameter region where the unpolarized quark matter is in the CSC phase. In Fig.7, we plot m and Δ against $\delta\mu$ for $(G_D/G_S, T, \mu) = (1.0, 50, 600)$ (cf. Fig. 2 (b)). As $\delta\mu$ increases, a phase transition occurs at $\delta\mu = \delta\mu_p$ and the quark matter turns out to the color normal phase, while (small) m is nearly independent of $\delta\mu$. We have carried out the same computation choosing different parameter values and found qualitatively the same results.

2. Thermodynamic potential

Here we compute the thermodynamic potential $\Omega(\mu, T; \delta\mu)$ as a function of $\delta\mu$, for different values of (μ, T), and discuss their physical implications.

Two typical behaviors of Ω are shown in Fig. 8. In the system with Ω as in the panel (a), the "polarized" or "ferromagnetic" phase is realized, and we refer such an Ω to as the "ferromagnetic (FM)" type. On the other hand, in the system with Ω as in the panel (b), the unpolarized phase is realized, and we refer such an Ω to as the "normal (N)" type.

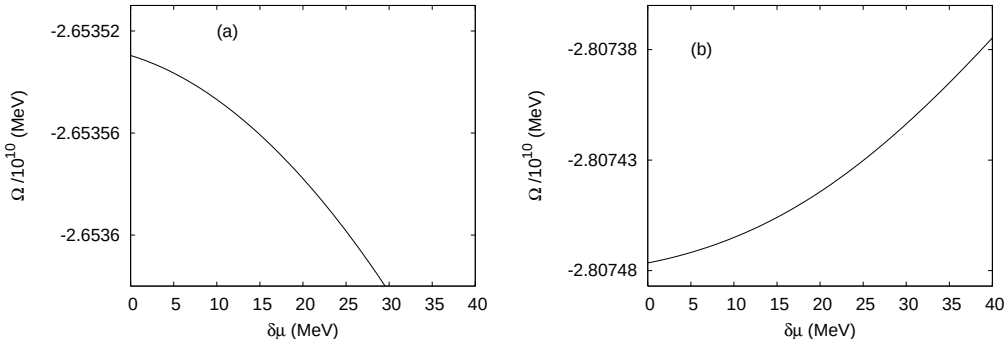

Fig. 8: Ω(T=0) against $\delta\mu$ for $\mu = 400$. The panels (a) and (b) correspond to $G_D/G_S = 3/4$ and 1.2, respectively.

Through numerical computation of Ω, we have found the following results.

1) For $G_D/G_S \lesssim 1.15$, Ω is of the FM-type in whole region of (μ, T). As an illustraion, we depict in Fig. 8 (a) $\Omega(\mu = 400, T = 0; \delta\mu)$ as a function of $\delta\mu$ for $G_D/G_S = 3/4$.

2) For $G_D/G_S \gtrsim 1.15$, there appears a window in the (μ, T)-plane, in which Ω is of the N-type. We show in Fig. 9 the phase diagrams in the (μ, T)-plane. The panel (a)

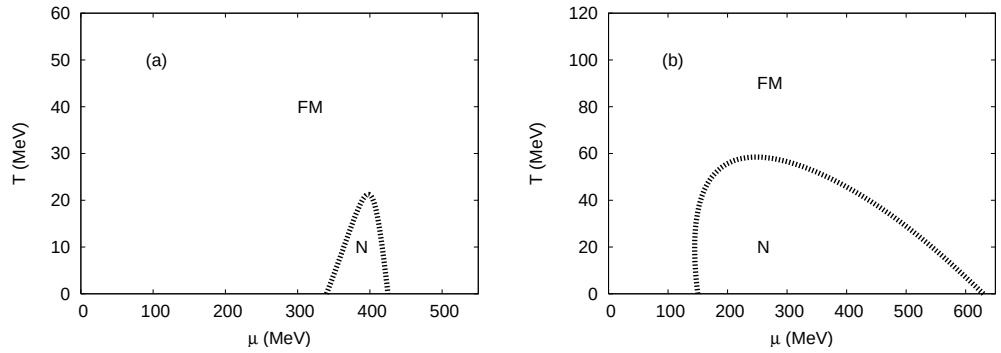

Fig. 9: Phase diagrams with respect to polarization. The panels (a) and (b) correspond to $G_D/G_S = 1.2$ and 1.5, respectively.

FM and N stand for the "ferromagnetic" and "normal" phase, respectively.

[(b)] corresponds to $G_D/G_S = 1.2$ [1.5]. As an illustration, we plot in Fig. 8 (b) $\Omega(\mu = 400, T = 0; \delta\mu)$ against $\delta\mu$ for $G_D/G_S = 1.2$, which is of the N-type.

To see how Ω changes through the transition region from the FM-type region to the N-type region, we display $\Omega(\mu = 330, T = 0; \delta\mu)$ and $\Omega(\mu = 340, T = 0; \delta\mu)$ for $G_D/G_S = 1.2$ in Figs. 10 (a) and (b), respectively. Fig. 10 (a) indicates that, for $(G_D/G_S, \mu, T) = (1.2, 330, 0)$, a metastable state appears at $\delta\mu = 0$, while Fig. 10 (b) shows that, for $(G_D/G_S, \mu, T) = (1.2, 340, 0)$, a stable state appears at intermediate $\delta\mu$.

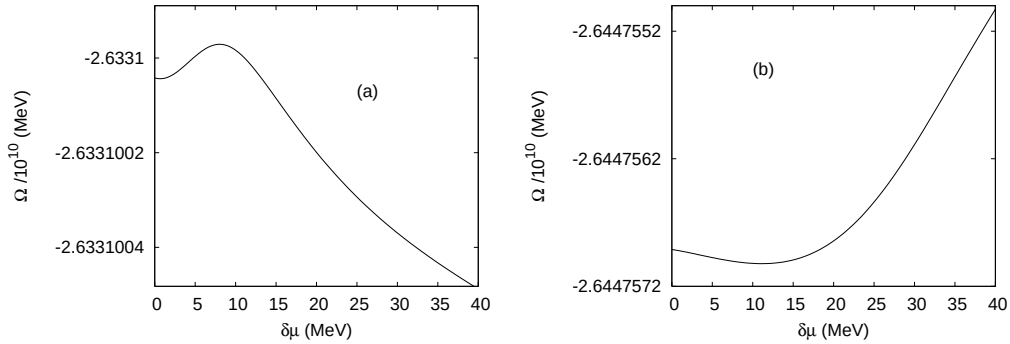

Fig. 10: Ω(T=0) against $\delta\mu$ for $G_D/G_S = 1.2$. The panels (a) and (b) correspond to $\mu = 330$ and 340, respectively.

Numerical analyses show that, in the region where $\Delta = 0$, Ω decreases as $\delta\mu$ increases, so that Ω is of the FM-type. Since $\Delta = 0$ at high temperature (cf. Figs. 3 and 4), Ω is of the FM-type at high T. For the normal phase to appear, $\Delta \neq 0$ is necessary.

V. SUMMARY AND DISCUSSION

In this paper, generalizing the analysis in [8], we have dealt with unpolarized and polarized two-flavor quark matters at zero and finite temperatures.

We have used the extended Nambu–Jona-Lassinio model and employed the mean-field approximation. The model contains two coupling constants, the quark-antiquark coupling constant G_S and the diquark coupling constant G_D. Although G_S and G_D have the relation $G_D = (3/4)G_S$, we have treated, as in [7], G_D/G_S as a free parameter.

The unpolarized case at $T = 0$ are fully analyzed in [7]. In addition to it, we have analyzed the unpolarized case at finite temperatures through computing the thermodynamic potential. The result is summarized as the phase diagrams in the (μ, T)-plane in Fig. 4. The structure of the diagrams are qualitatively the same for all values of G_D/G_S considered in this paper.

We have dealt with two types of polarized two-flavor quark matters, i.e., the "magnetic-moment"-polarized and the "spin"-polarized quark matters. For describing such systems, the extended Nambu–Jona-Lassionio model is generalized to treat the chiral condensate, diquark condensate, and the degree of polarization on an equal footing. We have shown that, within the mean-field approximation, the form of the thermodynamic potential Ω is the same for both the "magnetic-moment"-polarized and the "spin"-polarized cases.

We have found that, as in the cases of other quantities, the $\delta\mu$ dependence of Ω heavily depends on the value of G_D/G_S. For small $G_D/G_S \lesssim 1.15$, Ω is of the "ferromagnetic"-type, while, for large $G_D/G_S \gtrsim 1.15$, there appears a window in the (μ, T)-plane, where Ω is of the "normal"-type. We have found interesting behaviors of Ω in the transition regions between the "ferromagnetic"-type and the "normal"-type regions. We have seen that, at high temerature and/or density, the "ferromagnetic" phase is energetically favored over the "normal" phase, which is in conflict with intuition. This fact may suggests that the extended Nambu–Jona-Lasinio model supplemented with the mean-field approximation is not applicable to the polarized quark matter in such regions.

The analysis presented in this paper is the "first-stage analysis". Closer investigation is to be done in various directions. Among others, are 1) inclusion of the residual interactions, and 2) incorporation of electron, positron, and gluons into the NJL model. Also interesting is to apply the method in this paper to quark matters in different phases, such as the gapless

charge-neutral 2SC phase, the color-flavor-loced phase, the non-uniformly condensed phases [10], and so on.

APPENDIX A: THE ROLE OF THE PROJECTORS $\mathcal{P}_s^\tau$ $(\tau = \pm, s = \pm)$

We start with briefly reviewing the spin content of $q(x)$. We employ the box normalization by confining the system within a cube and introduce the periodic boundary condition to make the single-particle plane-wave basis. $q(x)$ in the interaction picture is expanded, in standard notations, as

$$q(x) = \sum_{\mathbf{p}} \sum_{s=\pm} \sqrt{\frac{m_0}{VE}} \left[a_s(\vec{p}) u_s(\vec{p}) e^{-ip\cdot x} + b_s^\dagger(\vec{p}) v_s(\vec{p}) e^{ip\cdot x} \right] ,$$

where $\mathcal{P}_s(\vec{p}) u_{s'}(\vec{p}) = \delta_{ss'} u_s(\vec{p})$ and $\mathcal{P}_s(\vec{p}) v_{s'}(\vec{p}) = \delta_{ss'} v_s(\vec{p})$. The third component of the spin operator reads $S^z = \frac{1}{2} \int d^3x\, q^\dagger(x) \sigma^3 q(x)$. Expectation values of S^z in one quark- and one antiquark- states are computed, in respective order, as (cf. [8])

$$\begin{aligned}
\langle 0 | a_\pm(\vec{p}) S^z a_\pm^\dagger(\vec{p}) | 0 \rangle &= \frac{m_0}{2E_p} u^\dagger(\vec{p}) \mathcal{P}_\pm^\dagger(\vec{p}) \sigma^3 \mathcal{P}_\pm(\vec{p}) u(\vec{p}) \\
&= \frac{1}{2} \mathrm{Tr} \left(\mathbf{P}_\pm^{(-)}(-\vec{p}) \sigma^3 \right) \\
&= \pm \frac{m_0}{2E_p} n^3(\vec{p}) \,, \qquad \text{(A.1)} \\
\langle 0 | b_\pm(\vec{p}) S^z a_\pm^\dagger(\vec{p}) | 0 \rangle &= -\frac{m_0}{2E_p} v^\dagger(\vec{p}) \mathcal{P}_\pm^\dagger(\vec{p}) \sigma^3 \mathcal{P}_\pm(\vec{p}) v(\vec{p}) \\
&= -\frac{1}{2} \mathrm{Tr} \left(\mathbf{P}_\pm^{(+)}(\vec{p}) \sigma^3 \right) \\
&= \pm \frac{m_0}{2E_p} n^3(\vec{p}) \,. \qquad \text{(A.2)}
\end{aligned}$$

The minus sign on the right-hand side of the first line in Eq. (A.2) comes from the fact that the quark obeys the Fermi-Dirac statistics. Then, we call the state with $\mathcal{P}_+(\vec{p}) = 1$ ($\mathcal{P}_+(\vec{p}) = -1$) the "spin up" ("spin down") state.

To see the role of $\mathbf{P}_s^{(\tau)}$, we first apply $\mathbf{P}_s^{(-)}(i\nabla)$ to $q(x)$,

$$\begin{aligned}
\mathbf{P}_s^{(-)}(i\nabla) q(x) &= \sum_{\mathbf{p}} \sum_{s'} \sqrt{\frac{m_0}{VE}} \Big[a_{s'}(\vec{p}) \mathcal{P}_s(\vec{p}) \tilde{\Lambda}_-(-\vec{p}) u_{s'}(\vec{p}) e^{-ip\cdot x} \\
&\quad + b_{s'}^\dagger(\vec{p}) \mathcal{P}_s(-\vec{p}) \tilde{\Lambda}_-(\vec{p}) v_{s'}(\vec{p}) e^{ip\cdot x} \Big] .
\end{aligned}$$

Noticing that $\tilde{\Lambda}_-(-\vec{p}) u_{s'}(\vec{p}) = u_{s'}(\vec{p})$ and $\tilde{\Lambda}_-(\vec{p}) v_{s'}(\vec{p}) = 0$, we have

$$\mathbf{P}_s^{(-)}(i\nabla) q(x) = \sum_{\mathbf{p}} \sqrt{\frac{m_0}{VE}} a_s(\vec{p}) u_s(\vec{p}) e^{-ip\cdot x} .$$

Thus $\mathbf{P}^{(-)}_{\pm}(i\nabla)$ projects out onto the "spin-up" ("spin-down") positive energy-state. Similarly, using $\tilde{\Lambda}_+(-\vec{p})u_{s'}(\vec{p}) = 0$ and $\tilde{\Lambda}_+(\vec{p})v_{s'}(\vec{p}) = v_{s'}(\vec{p})$, we have

$$\mathbf{P}^{(+)}_{s}(i\nabla)q(x) = \sum_{\mathbf{p}} \sqrt{\frac{m_0}{VE}} b^{\dagger}_{s}(\vec{p})v_s(\vec{p})e^{ip\cdot x}$$

and then $\mathbf{P}^{(+)}_{\pm}(i\nabla)$ projects out onto the "spin-up" ("spin-down") negative energy-state.

APPENDIX B: CONSERVATION OF Q_+ AND Q_- UP TO $O(G_s)$ AND $O(G_D)$

In this Appendix, we show that both the "magnetic-moment (MM)"-polarized net quark-number charges (Q_+ and Q_-) and the "spin"-polarized ones (Q'_+ and Q'_-) are conserved up to and including $O(G_S)$ and $O(G_D)$.

The Hamiltonian reads

$$\begin{aligned} H(x_0) &= \int d^3x \mathcal{H}(x) \equiv H_0 + H_S + H_{PS} + H_D \,, \qquad \text{(B.1)} \\ \mathcal{H} &= \bar{q}\left(-i\vec{\gamma}\cdot\nabla + m_0\right)q - G_S\left[(\bar{q}q)^2 + (\bar{q}i\gamma_5\vec{\tau}q)^2\right] , \\ &\quad -G_D\left[\left(i\bar{q}^C\epsilon\epsilon^b\gamma_5 q\right)\left(i\bar{q}\epsilon\epsilon^b\gamma_5 q^C\right)\right] . \qquad \text{(B.2)} \end{aligned}$$

Here H_0, H_S, H_{PS}, and H_D are, in respective order, the free-, the scalar quark-antiquark interaction, the pseudoscalar quark-antiquark interaction, and the diquark interaction Hamiltonians. Since $Q_\pm = Q^{(-)}_\pm + Q^{(+)}_\mp$ and $Q'_\pm = Q^{(-)}_\pm + Q^{(+)}_\pm$, it is sufficient to show that $\left[H(x_0), Q^{(\tau)}_s(x_0)\right] = O(G_S^2, G_D^2, G_S G_D)$.

The quark propagator G in the imaginary-time formalism is $G_{11}\Big|_{|\Delta|=0}$ with m_0 for m, where G_{11} is as in Appendix C:

$$G = \begin{cases} \displaystyle\sum_{\tau,\, s=\pm} \frac{\gamma_0 \mathbf{P}^{(\tau)}_s(\vec{p})}{p_0 + \tau E_p + \mu_{-\tau s}} & (\text{"MM"-polarized case}) \,, \\ \displaystyle\sum_{\tau,\, s=\pm} \frac{\gamma_0 \mathbf{P}^{(\tau)}_s(\vec{p})}{p_0 + \tau E_p + \mu_{s}} & (\text{"spin"-polarized case}) \,, \end{cases} \qquad \text{(B.3)}$$

where $p_0 = ip_{0E}$.

Derivation of $\left[H_0,\, Q_s^{(\tau)}\right] = 0$

We write H_0 as

$$\begin{aligned} H_0 &= \int d^3x\, \bar{q}\,(-i\vec{\gamma}\cdot\nabla + m_0)\, q \\ &= \int d^3x\, q^\dagger E \sum_s \left[\mathbf{P}_s^{(-)}(i\nabla) - \mathbf{P}_s^{(+)}(i\nabla)\right] q\,, \end{aligned}$$

where $E \equiv \sqrt{-\nabla^2 + m_0^2}$. Using Eq. (2.6), we can easily show that the equal-time commutator between $Q_s^{(\tau)}$ and H_0 vanishes:

$$\left[Q_s^{(\tau)},\, H_0\right] = 0\,.$$

Derivation of $\left[H_{S(PS)},\, Q_s^{(\tau)}\right] = O(G_S^2, G_D^2, G_D G_S)$

We start with computing

$$\begin{aligned} \left[H_{S(PS)},\, Q_s^{(\tau)}\right] &= G_S \int d^3x \left[\left(\bar{q}\left[\mathbf{P}_s^{(\tau)}(i\overleftarrow{\nabla})\Gamma - \Gamma\mathbf{P}_s^{(\tau)}(i\nabla)\right] q\right)(\bar{q}\Gamma q) \right. \\ &\quad \left. + (\bar{q}\Gamma q)\left(\bar{q}\left[\mathbf{P}_s^{(\tau)}(i\overleftarrow{\nabla})\Gamma - \Gamma\mathbf{P}_s^{(\tau)}(i\nabla)\right] q\right)\right]\,, \end{aligned} \tag{B.4}$$

where $\Gamma = 1$ for H_S and $\Gamma = i\gamma_5\vec{\tau}$ for H_{PS}.

Let us compute the ensemble average of Eq. (B.4) up to $O(G_S)$ using Eq. (B.3):

$$\begin{aligned} \left\langle\left[H_{S(PS)},\, Q_s^{(\tau)}\right]\right\rangle &= 2G_S V T^2 \sum_{p_0,\, q_0} \int \frac{d^3p}{(2\pi)^3} \int \frac{d^3q}{(2\pi)^3} \\ &\quad \times \mathrm{Tr}\left[G(\vec{q})\left\{\Gamma\mathbf{P}_s^{(\tau)}(-\vec{p}) - \mathbf{P}_s^{(\tau)}(\vec{q})\Gamma\right\} G(\vec{p})\Gamma\right]\,, \end{aligned} \tag{B.5}$$

where V is the volume of the system. Appropriate regurarization is understood to be introduced. From Eq. (B.3), we have

$$\mathbf{P}_s^{(\tau)}(-\vec{p})G(\vec{p}) = G(\vec{p})\mathbf{P}_s^{(\tau)}(\vec{p})\,. \tag{B.6}$$

Using this relation in Eq. (B.5), one can readily see that the right-hand side vanishes, so that $\left[H_{S(PS)},\, Q_s^{(\tau)}\right] = O(G_S^2, G_D^2, G_S G_D)$.

Derivation of $\left[H_D,\, Q_s^{(\tau)}\right] = 0(G_S^2, G_D^2, G_D G_S)$

We start with computing

$$\begin{aligned}\left[H_D,\, Q_s^{(\tau)}\right] \;=\; 2G_D \int d^3x \,\big[&\left(\bar{q}^C \epsilon\epsilon^b \gamma_5 \mathbf{P}_s^{(\tau)}(i\nabla) q\right)\left(\bar{q}\epsilon\epsilon^b\gamma_5 q^C\right) \\ &- \left(\bar{q}^C\epsilon\epsilon^b\gamma_5 q\right)\left(\bar{q}\mathbf{P}_s^{(\tau)}(i\overleftarrow{\nabla})\epsilon\epsilon^b\gamma_5 q^C\right)\big]\,. \end{aligned} \tag{B.7}$$

Computation of the ensemble average of Eq. (B.7) up to $O(G_D)$ yields

$$\begin{aligned}\left\langle\left[H_D,\, Q_s^{(\tau)}\right]\right\rangle \;=\; 16 G_D V T^2 \sum_{p_0,\,q_0}\int\frac{d^3p}{(2\pi)^3}\int\frac{d^3q}{(2\pi)^3} \\ \times \mathrm{Tr}\left[G^T(\vec{q})C\gamma_5\left\{\mathbf{P}_s^{(\tau)}(-\vec{p})G(\vec{p}) - G(\vec{p})\mathbf{P}_s^{(\tau)}(\vec{p})\right\}\gamma_5 C\right]\,. \end{aligned} \tag{B.8}$$

Using the relation (B.6) in Eq. (B.8), one can readily see that the right-hand side vanishes, so that $\left[H_D,\, Q_s^{(\tau)}\right] = O(G_S^2, G_D^2, G_S G_D)$.

APPENDIX C: PROPAGATORS

In this Appendix, for completeness, we write down the form of propagator G with G^{-1} as in Eq. (3.10). The propagator G_0 for the blue quark is obtained from G by taking the limit $\Delta \to 0$ and deleting $\mathbf{1}_c^{\perp}$.

Magnetic-moment–polarized quark matter

Straightforward manipulation yields, with obvious notation,

$$\begin{aligned} G_{11(22)} \;=\; &\sum_s \left[\frac{p_0 - E_p \mp \mu_{\pm s}}{(p_0 + E_p \pm \mu_{\mp s})(p_0 - E_p \mp \mu_{\pm s}) - |\Delta|^2}\gamma_0 \mathbf{P}_s^{(+)}(\vec{p})\right. \\ &\left. + \frac{p_0 + E_p \mp \mu_{\mp s}}{(p_0 - E_p \pm \mu_{\pm s})(p_0 + E_p \mp \mu_{\mp s}) - |\Delta|^2}\gamma_0 \mathbf{P}_s^{(-)}(\vec{p})\right]\mathbf{1}_f\mathbf{1}_c^{\perp}\,, \\ G_{21(12)} \;=\; &\sum_s \frac{\Delta^{\pm}}{(p_0 + E_p \pm \mu_{\mp s})(p_0 - E_p \mp \mu_{\pm s}) - |\Delta|^2}\mathbf{P}_s^{(+)}(\vec{p}) \\ &+ \frac{\Delta^{\pm}}{(p_0 - E_p \pm \mu_{\pm s})(p_0 + E_p \mp \mu_{\mp s}) - |\Delta|^2}\mathbf{P}_s^{(-)}(\vec{p})\,, \end{aligned}$$

where $p_0 = i p_{0E}$.

The propagator G is deduced as

$$\begin{aligned} G_{11(22)} &= \sum_s \left[\frac{p_0 - E_p \mp \mu_{-s}}{(p_0 + E_p \pm \mu_s)(p_0 - E_p \mp \mu_{-s}) - |\Delta|^2} \gamma_0 \mathbf{P}_s^{(+)}(\vec{p}) \right. \\ &\quad \left. + \frac{p_0 + E_p \mp \mu_{-s}}{(p_0 - E_p \pm \mu_s)(p_0 + E_p \mp \mu_{-s}) - |\Delta|^2} \gamma_0 \mathbf{P}_s^{(-)}(\vec{p}) \right] \mathbf{1}_f \mathbf{1}_c^{\perp} \,, \\ G_{21(12)} &= \sum_s \frac{\Delta^{\pm}}{(p_0 + E_p \pm \mu_s)(p_0 - E_p \mp \mu_{-s}) - |\Delta|^2} \mathbf{P}_s^{(+)}(\vec{p}) \\ &\quad + \frac{\Delta^{\pm}}{(p_0 - E_p \pm \mu_s)(p_0 + E_p \mp \mu_{-s}) - |\Delta|^2} \mathbf{P}_s^{(-)}(\vec{p}) \,. \end{aligned}$$

APPENDIX D: DERIVATION OF EQ. (3.13)

In this Appendix, we compute $\mathrm{Det}\left(-\beta G^{-1}\right)$ in Eq. (3.12) with Eq. (3.10),

$$\mathrm{Det}\left(-\beta G^{-1}\right) = \mathrm{Det}\left[-\beta \begin{pmatrix} \left(G_0^{+}\right)^{-1} \mathbf{1}_f \mathbf{1}_c^{\perp} & \Delta^{-} \\ \Delta^{+} & \left(G_0^{-}\right)^{-1} \mathbf{1}_f \mathbf{1}_c^{\perp} \end{pmatrix} \right] .$$

Using the identities,

$$\mathrm{Det} \begin{pmatrix} A & B \\ C & D \end{pmatrix} = (-)^n \mathrm{Det}\left(CB - CAC^{-1}D\right) = (-)^n \mathrm{Det}\left(BC - BDB^{-1}A\right) \,, \qquad \text{(D.1)}$$

where A, B, C, and D are $(n \times n)$ matrices, we obtain

$$\begin{aligned} \left[\mathrm{Det}\left(-\beta G^{-1}\right)\right]^2 &= \mathrm{Det}\left\{ \beta^4 \prod_{\tau=\pm} \left[\Delta^{\tau}\Delta^{-\tau} - \Delta^{\tau} \left(G_0^{\tau}\right)^{-1} \left(\Delta^{\tau}\right)^{-1} \left(G_0^{-\tau}\right)^{-1} \right] \right\} \\ &= \mathrm{Det}\left\{ \beta^4 \prod_{\tau=\pm} \left[-|\Delta|^2 - \gamma_5 \left(G_0^{\tau}\right)^{-1} \gamma_5 \left(G_0^{-\tau}\right)^{-1} \right] \mathbf{1}_f \mathbf{1}_c^{\perp} \right\} \,, \qquad \text{(D.2)} \end{aligned}$$

where use has been made of Eq. (3.7).

Substituting Eq. (3.8) into Eq. (D.2), and using Eqs. (2.7), (2.8), and (2.6) we obtain, after some algebras,

$$\begin{aligned} \left[\mathrm{Det}\left(-\beta G^{-1}\right)\right]^2 &= \mathrm{Det}\left[\beta^4 \left\{ F_1 - 2p_0 \left(p_0^2 - E_p^2 - \mu_+\mu_- - |\Delta|^2 \right) \right. \right. \\ &\quad \left. \left. \times \sum_s \left(\mu_s - \mu_{-s}\right) \left(\mathbf{P}_s^{(+)}(-\vec{p}) - \mathbf{P}_s^{(-)}(-\vec{p}) \right) \right\} \mathbf{1}_f \mathbf{1}_c^{\perp} \right] \,, \end{aligned}$$

where $p_0 = ip_{0E}$ (cf. Eq. (3.9)) and

$$F_1 = \left(p_0^2 - E_p^2 - \mu_+\mu_- - |\Delta|^2\right)^2 + p_0^2\left(\mu_+ - \mu_-\right)^2 - E_p^2\left(\mu_+ + \mu_-\right)^2 \, .$$

Using Eq. (2.5) with Eqs. (2.3) and (2.4), and Eq. (2.2), we obtain, after some algebras,

$$\left[\mathrm{Det}\left(-\beta G^{-1}\right)\right]^2 = \mathrm{Det}\beta^4 \begin{pmatrix} F_{11} & F_{12} \\ F_{21} & F_{22} \end{pmatrix} \, .$$

Here

$$\begin{aligned} F_{11} &= F_{22} = \left[F_1 \mathbf{1}_2 + \frac{m}{E_p}\left(\vec{\sigma}\cdot\vec{n}\right)F_2\right]\mathbf{1}_2\mathbf{1}_f\mathbf{1}_c^{\perp} \, , \\ F_{12} &= -F_{21} \equiv -\frac{i}{E_p}\left[\left(\vec{p}\times\vec{n}\right)\cdot\vec{\sigma}\, F_2\right]\mathbf{1}_f\mathbf{1}_c^{\perp} \, , \end{aligned}$$

where $\vec{n} = \vec{n}(\vec{p})$, $\mathbf{1}_2$ is the (2×2) unit matrix in a spin space, and

$$F_2 = 2p_0\left(\mu_+ - \mu_-\right)\left(p_0^2 - E_p^2 - \mu_+\mu_- - |\Delta|^2\right) \, .$$

Using Eq. (D.1) again, we obtain, after some algebras,

$$\left[\mathrm{Det}\left(-\beta G^{-1}\right)\right]^2 = \mathrm{Det}\left\{\beta^8\left(F_2^2 - F_1^2\right)\mathbf{1}_2\mathbf{1}_f\mathbf{1}_c^{\perp}\right\} \, ,$$

where use has been made of $|\vec{p}\times\vec{n}| = \vec{p}^{\,2}\vec{n}^{\,2} - (\vec{p}\cdot\vec{n})^2$ and Eq. (2.2). Further manipulation yields (cf. Eq. (3.12))

$$\ln \mathcal{Z}_{r,g} = \frac{1}{2}\ln \mathrm{Det}\left(-\beta G^{-1}\right) = N_f \sum_n \sum_{\vec{p}} \ln\left(\prod_{\rho=\pm}\prod_{\sigma=\pm}\left[p_0^2 - \left(E_{p,\,\rho}^{(\sigma)}\right)^2\right]\right)$$

with

$$E_{p,\,\rho}^{(\sigma)} = \left[\left(E_p + \sigma\frac{\mu_+ + \mu_-}{2}\right)^2 + |\Delta|^2\right]^{1/2} + \rho\frac{\mu_+ - \mu_-}{2} \, . \tag{D.3}$$

Using the relation

$$\sum_n \ln\left[\beta^2\left(p_0^2 - E^2\right)\right] = \beta\left[E + 2T\ln\left(1 + e^{-\beta E}\right)\right]$$

and making the replacement being valid in the large-V limit,

$$\sum_n \to V\int\frac{d^3p}{(2\pi)^3} \, ,$$

we finally obtain for the contribution from the red- and green-quarks to the thermodynamic potential,

$$\begin{aligned}\Omega_{r,\,g} &\equiv -T\frac{\ln \mathcal{Z}_{r,\,g}}{V} \\ &= -N_f \int \frac{d^3p}{(2\pi)^3} \sum_{\rho,\,\sigma=\pm} \left[E_{p,\,\rho}^{(\sigma)} + 2T \ln\left(1 + e^{-\beta E_{p,\,\rho}^{(\sigma)}}\right)\right] . \end{aligned} \tag{D.4}$$

[1] S. C. Frautschi, Proc. of the Workshop on Hadronic Matter at Extreme Energy Density, N. Cabbibo (ed.), Erice, Italy (1978); F. Barrois, Nucl. Phys. **B129**, 390 (1977); D. Balin and A. Love, Nucl. Phys. **B190**, 175 (1981).

[2] R. Rapp, T. Schäfer, E. V. Shuryak, and M. Velkovsky, Phys. Rev. Lett. **81**, 53 (1998); M. Alford, K. Rajagopal, and F. Wilzek, Phys. Lett. **B422**, 247 (1998).

[3] Y. Nambu and G. Jona-Lasinio, Phys. Rev. **112**, 345 (1961); **124**, 246 (1961).

[4] T. Hatsuda and T. Kunihiro, Phys. Rep. **247**, 221 (1994).

[5] T. M. Schwarz, S. P. Klevansky, and G. Papp, Phys. Rev. C **60**, 055205 (1999); B. Vanderheyden and A. D. Jackson, Phys. Rev. D **62**, 094010 (2000).

[6] D. H. Rischke, Prog. Nucl. Phys. **52**, 197 (2004); K. Rajagopal and F. Wilczek, hep-ph/0011333; D. K. Hong, Acta Phys. Polon. B **32**, 1253 (2001); M. Alford, Ann. Rev. Nucl. Part. Sci. **51**, 131 (2001); G. Nardulli, Riv. Nuovo Cim. **25N3**, 1 (2002); T. Schäfer, hep-ph/0304281; M. Buballa, Phys. Rep. **407**, 205 (2005); H. C. Ren, hep-ph/0404074.

[7] M. Huang, Int. J. Mod. Phys. E **14**, 675 (2005).

[8] T. Tatsumi, Phys. Lett. **B489**, 280 (2000).

[9] E. Nakano, T. Maruyama, and T. Tatsumi, Phys. Rev. D **68**, 105001 (2003); T. Tatsumi, T. Maruyama, and E. Nakano, Prog. Theor. Phys. Suppl. **153**, 190 (2004); A. Niégawa, Prog. Theor. Phys. **113**, 581 (2005); T. Tatsumi, E. Nakano, and K. Nawa, hep-ph/0506002; T. Tatsumi, T. Maruyama, K. Nawa, and E. Nakano, hep-ph/0502201; S. Maedan, hep-ph/0605311; T. Tatsumi, T. Maruyama, E. Nakano, and K. Nawa, Nucl. Phys. **A 774**, 827 (2006); K. Ohnishi, M. Oka, and S. Yasui, hep-ph/0609060.

[10] M. Sadzikowski, Phys. Lett. **B642**, 238 (2006).